

¹ The human visual system preserves the hierarchy
² of 2-dimensional pattern regularity

³ Peter J. Kohler^{1,2,3} and Alasdair D. F. Clarke⁴

⁴ *¹ York University, Department of Psychology, Toronto, ON M3J 1P3, Canada*

⁵ *² Centre for Vision Research, York University, Toronto, ON, M3J 1P3, Canada*

⁶ *³ Stanford University, Department of Psychology, Stanford, CA 94305, United States*

⁷ *⁴ University of Essex, Department of Psychology, Colchester, UK, CO4 3SQ*

⁸ **Abstract**

Symmetries are present at many scales in natural scenes. Humans and other animals are highly sensitive to visual symmetry, and symmetry contributes to numerous domains of visual perception. The four fundamental symmetries, reflection, rotation, translation and glide reflection, can be combined into exactly 17 distinct regular textures. These *wallpaper groups* represent the complete set of symmetries in 2D images. The current study seeks to provide a more comprehensive description of responses to symmetry in the human visual system, by collecting both brain imaging (Steady-State Visual Evoked Potentials measured using high-density EEG) and behavioral (symmetry detection thresholds) data using the entire set of wallpaper groups. This allows us to probe the hierarchy of complexity among wallpaper groups, in which simpler groups are subgroups of more complex ones. We find that both behavior and brain activity preserve the hierarchy almost perfectly: Subgroups consistently produce lower amplitude symmetry-specific responses in visual cortex and require longer presentation durations to be reliably detected. These findings expand our understanding of symmetry perception by showing that the human brain encodes symmetries with a high level of precision and detail. This opens new avenues for research on how fine-grained representations of regular textures contribute to natural vision.

Symmetries are abundant in natural and man-made environments, due to a complex interplay of physical forces that govern pattern formation in nature. Sensitivity to symmetry has been demonstrated in a number of species, includes bees (Giurfa et al., 1996), fish (Morris and Casey, 1998; Schlüter et al., 1998), birds (Møller, 1992; Swaddle and Cuthill, 1994) and dolphins (von Fersen et al., 1992), and may be used as a cue for mate selection in many species (Swaddle, 1999) including humans (Rhodes et al., 1998). Humans cultures have created and appreciated symmetrical patterns throughout history, and since the gestalt movement of the early 20th century, symmetry has been recognized as important for visual perception. Symmetry contributes to the perception of shapes (Palmer, 1985; Li et al., 2013), scenes (Apthorp and Bell, 2015) and surface properties (Cohen and Zaidi, 2013). This literature is almost exclusively based on stimuli in which one or more symmetry axes are placed at a single point in the image. Focus has been on mirror symmetry or reflection, with relatively few studies including the other fundamental

37 symmetries: *rotation*, *translation* and *glide reflection* (Wagemans, 1998) - perhaps because reflection
38 has been found to be more perceptually salient (Mach, 1959; Royer, 1981; Palmer, 1991; Ogden
39 et al., 2016; Hamada and Ishihara, 1988) and produce more brain activity (Makin et al., 2013, 2014,
40 2012; Wright et al., 2015). In the current study, we take a different approach by investigating
41 visual processing of regular textures in which combinations of the four fundamental symmetries
42 tile the 2D plane.

43 In the two spatial dimensions relevant for images, symmetries can be combined in 17 distinct
44 ways, *the wallpaper groups* (Fedorov, 1891; Polya, 1924; Liu et al., 2010). Previous work on a subset
45 of four of the wallpaper groups used functional MRI to demonstrate that rotation symmetries
46 in wallpapers elicit parametric responses in several areas in occipital cortex, beginning with
47 visual area V3 (Kohler et al., 2016). This effect was also robust when symmetry responses were
48 measured with electroencephalography (EEG) using both Steady-State Visual Evoked Potentials
49 (SSVEPs)(Kohler et al., 2016) and Event-Related Potentials (Kohler et al., 2018). The SSVEP
50 technique uses periodic visual stimulation to produce a periodic brain response that is confined to
51 integer multiples of the stimulation frequency known as harmonics. SSVEP response harmonics
52 can be isolated in the frequency domain and depending on the specific design, different harmonics
53 will express different aspects of the brain response. (Norcia et al., 2015). Here we extend on the
54 previous work by collecting SSVEPs and psychophysical data from human participants viewing
55 the full set of wallpaper groups. We measure responses in visual cortex to 16 out of the 17
56 wallpaper groups, with the 17th serving as a control stimulus. Our goal is to provide a more
57 complete picture of how wallpaper groups are represented in the human visual system.

58 A wallpaper group is a topologically discrete group of isometries of the Euclidean plane, i.e.
59 transformations that preserve distance (Liu et al., 2010). The wallpaper groups differ in the
60 number and kind of these transformations and we can uniquely refer to different groups using
61 crystallographic notation. In brief, most groups are notated by PXZ , where $X \in \{1, 2, 3, 4, 6\}$
62 indicates the highest order of rotation symmetry and $Z \in \{m, g\}$ indicates whether the pattern
63 contains reflection (m) or glide reflection (g). For example, $P4$ contains rotation of order 4, while
64 $P4MM$ contains rotation of order 4 and two reflections. By convention, many of the groups
65 are given shortened names: for example, $P4MM$ is usually referred to as $P4M$, as the second
66 reflection can be deduced from the presence of rotation of order 4 alongside a reflection. Two of
67 the groups start with a C rather than a P , (CM and CMM) which indicates that the symmetries
68 are specified relative to a cell that itself contains repetition. Full details of the naming convention
69 can be found on wikipedia and examples of the wallpaper groups are shown in Figures 1 and 2.

70 In mathematical group theory, when the elements of one group is completely contained in
71 another, the inner group is called a subgroup of the outer group (Liu et al., 2010). The full list
72 of subgroup relationships is listed in Section 1.4.2 of the Supplementary Material. Subgroup
73 relationships between wallpaper groups can be distinguished by their indices. The index of a
74 subgroup relationship is the number of cosets, i.e. the number of times the subgroup is found
75 in the supergroup (Liu et al., 2010). As an example, let us consider groups P_2 and P_6 (see Figure
76 1B). If we ignore the translations in two directions that both groups share, group P_6 consists
77 of the set of rotations $\{0^\circ, 60^\circ, 120^\circ, 180^\circ, 240^\circ, 300^\circ\}$, in which $P_2 \{0^\circ, 180^\circ\}$ is contained. P_2

78 is thus a subgroup of P_6 , and P_6 can be generated by combining P_2 with rotations $\{0^\circ, 120^\circ, 240^\circ\}$. Because P_2 is repeated three times in P_6 , P_2 is a subgroup of P_6 with index 3 (Liu et al., 2010). Similarly, PMM contains two reflections and rotations $\{0^\circ, 180^\circ\}$. PMM can be generated by adding an additional reflection to both P_2 ($\{0^\circ, 180^\circ\}$) and PM (one reflection), so P_2 and PM are both subgroups of PMM with index 2 (see Figure 1C). The 17 wallpaper groups thus obey a hierarchy of complexity where simpler groups are subgroups of more complex ones (Coxeter and Moser, 1972).

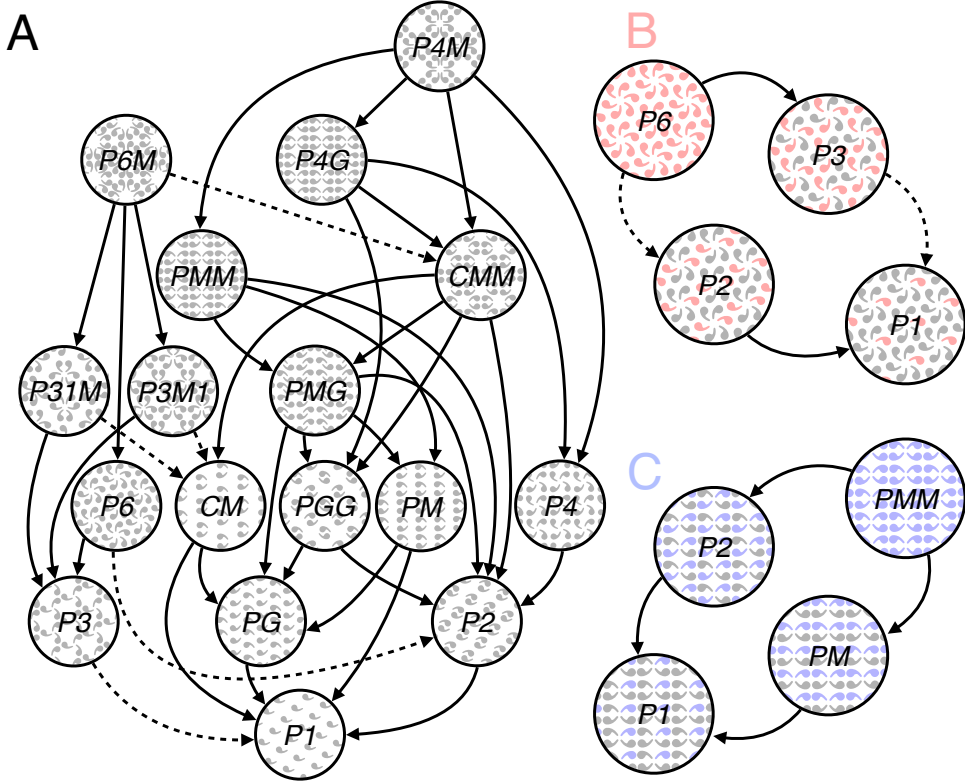


Figure 1: Subgroup relationships with indices 2 (solid lines) and 3 (dashed line) are shown in (A). All other relationships can be inferred by identifying the shortest path through the hierarchy, and multiplying the subgroup indices. For example, P_1 is related to P_6 through $P_6 \rightarrow P_3$ (index 2) and $P_3 \rightarrow P_1$ (index 3) so P_1 is also a subgroup of P_6 with index $3 \times 2 = 6$. We also show enlarged versions of some of the subgroup relationships involving P_6 (B, shown in red) and PMM (C, shown in blue) and highlight the symmetries within the subgroups to emphasize how the supergroup can be generated by adding additional transformations to the subgroup.

85 The two datasets we present here make it possible to assess the extent to which both behavior
 86 and brain responses follow the hierarchy of complexity expressed by the subgroup relationships.
 87 Based on previous brain imaging work showing that patterns with more axes of symmetry pro-
 88 duce greater activity in visual cortex (Sasaki et al., 2005; Tyler et al., 2005; Kohler et al., 2018,
 89 2016; Keefe et al., 2018), we hypothesized that more complex groups would produce larger SSVEPs.
 90 For the psychophysical data, we hypothesized that more complex groups would lead to shorter
 91 symmetry detection thresholds, based on previous data showing that under a fixed presentation
 92 time, discriminability increases with the number of symmetry axes in the pattern (Wagemans
 93 et al., 1991). Our results confirm both hypotheses, and show that activity in human visual cortex

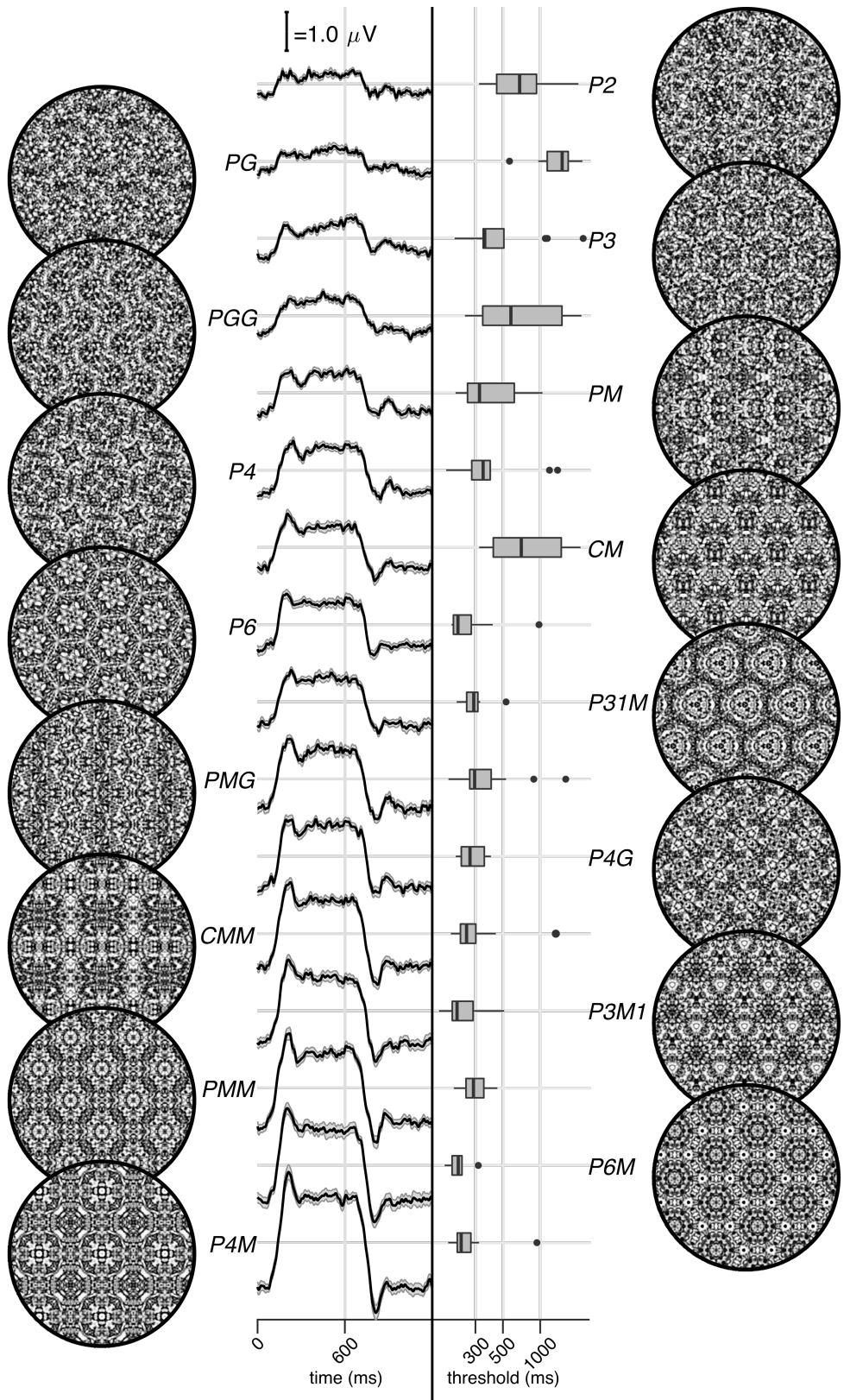


Figure 2: Examples of each of the 16 wallpaper groups are shown in the left- and right-most column of the figures, next to the corresponding SSVEP (center-left) and psychological (center-right) data from each group. The SSVEP data are odd-harmonic-filtered cycle-average waveforms. In each cycle, a P_1 exemplar was shown for the first 600 ms, followed by the original exemplar for the last 600 ms. Errorbars are standard error of the mean. Psychophysical data are presented as boxplots reflecting the distribution of display duration thresholds. The 16 groups are ordered by the strength of the SSVEP response, to highlight the range of response amplitudes.

is remarkably consistent with the hierarchical relationships between the wallpaper groups, with SSVEP amplitudes and psychophysical thresholds following these relationships at a level that is far beyond chance. The human visual system thus appears to encode all of the fundamental symmetries using a representational structure that closely approximates the subgroup relationships from group theory.

Results

The stimuli used in our two experiments were generated from random-noise textures, which made it possible to generate multiple exemplars from each of the wallpaper groups, as described in detail elsewhere (Kohler et al., 2016). We generated control stimuli matched to each exemplar in the main stimulus set, by scrambling the phase but maintaining the power spectrum. All wallpaper groups are inherently periodic because of their repeating lattice structure. Phase scrambling maintains this periodicity, so the phase-scrambled control images all belong to group P_1 regardless of group membership of the original exemplar. P_1 contains no symmetries other than translation, while all other groups contain translation in combination with one or more of the other three fundamental symmetries (reflection, rotation, glide reflection) (Liu et al., 2010). In our SSVEP experiment, this stimulus set allowed us to isolate brain activity specific to the symmetry structure in the exemplar images from activity associated with modulation of low-level features, by alternating exemplar images and control exemplars. In this design, responses to structural features beyond the shared power spectrum, including any symmetries other than translation, are isolated in the odd harmonics of the image update frequency (Kohler et al., 2016; Norcia et al., 2015, 2002). Thus, the combined magnitude of the odd harmonic response components can be used as a measure of the overall strength of the visual cortex response.

The psychophysical experiment took a distinct but related approach. In each trial an exemplar image was shown with its matched control, one image after the other, and the order varied pseudorandomly such that in half the trials the original exemplar was shown first, and in the other half the control image was shown first. After each trial, participants were instructed to indicate whether the first or second image contained more structure. The duration of both images was controlled by a staircase procedure so that a threshold duration for symmetry detection could be computed for each wallpaper group.

Examples of the wallpaper groups and a summary of our brain imaging and psychophysical measurements are shown in Figure 2. For our primary SSVEP analysis, we only considered EEG data from a pre-determined region-of-interest (ROI) consisting of six electrodes over occipital cortex (see Supplementary Figure 1.1). SSVEP data from this ROI was filtered so that only the odd harmonics that capture the symmetry response contribute to the waveforms. While waveform amplitude is quite variable among the 16 groups, all groups have a sustained negative-going response that begins at about the same time for all groups, 180 ms after the transition from the P_1 control exemplar to the original exemplar. To reduce the amplitude of the symmetry-specific response to a single number that could be used in further analyses and compared to the psychophysical data, we computed the root-mean-square (RMS) over the odd-harmonic-filtered waveforms. The data

in Figure 2 are shown in descending order according to RMS. The psychophysical results, shown in box plots in Figure 2, were also quite variable between groups, and there seems to be a general pattern where wallpaper groups near the top of the figure, that have lower SSVEP amplitudes, also have longer psychophysical threshold durations.

We now wanted to test our two hypotheses about how SSVEP amplitudes and threshold durations would follow subgroup relationships, and thereby quantify the degree to which our two measurements were consistent with the group theoretical hierarchy of complexity. We tested each hypothesis using the same approach. We first fitted a Bayesian model with wallpaper group as a factor and participant as a random effect. We fit the model separately for SSVEP RMS and psychophysical data and then computed posterior distributions for the difference between supergroup and subgroup. These difference distributions allowed us to compute the conditional probability that the supergroup would produce (a) larger RMS and (b) a shorter threshold durations, when compared to the subgroup. The posterior distributions are shown in Figure 3 for the SSVEP data, and in Figure 4 for the psychophysical data, which distributions color-coded according to conditional probability. For both data sets our hypothesis is confirmed: For the overwhelming majority of the 63 subgroup relationships, supergroups are more likely to produce larger symmetry-specific SSVEPs and shorter symmetry detection threshold durations, and in most cases the conditional probability of this happening is extremely high.

We also ran a control analysis using (1) odd-harmonic SSVEP data from a six-electrode ROI over parietal cortex (see Supplementary Figure 1.1) and (2) even-harmonic SSVEP data from the same occipital ROI that was used in our primary analysis. By comparing these two control analysis to our primary SSVEP analysis, we can address the specify of our effects in terms of location (occipital cortex vs parietal cortex) and harmonic (odd vs even). For both control analyses (plotted in Supplementary Figures 3.3 and 3.4), the correspondence between data and subgroup relationships was substantially weaker than in the primary analysis. We can quantify the strength of the association between the data and the subgroup relationships, by asking what proportion of subgroup relationships that reach or exceed a range of probability thresholds. This is plotted in Figure 5, for our psychophysical data, our primary SSVEP analysis and our two control SSVEP analyses. It shows that odd-harmonic SSVEP data from the occipital ROI and symmetry detection threshold durations both have a strong association with the subgroup relationships such that a clear majority of the subgroups survive even at the highest threshold we consider ($p(\Delta > 0 | data) > 0.99$). The association is far weaker for the two control analyses.

SSVEP data from four of the wallpaper groups (P_2 , P_3 , P_4 and P_6) was previously published as part of our earlier demonstration of parametric responses to rotation symmetry in wallpaper groups (Kohler et al., 2016). We replicate that result using our Bayesian approach, and find an analogous parametric effect in the psychophysical data (see Supplementary Figure 4.1). We also conducted an analysis testing for an effect of index in our two datasets and found that subgroup relationships with higher indices tended to produce greater pairwise differences between the subgroup and supergroup, for both SSVEP RMS and symmetry detection thresholds (see Supplementary Figure 4.2). The effect of index is relatively weak, but the fact that there is a measurable index effect can nonetheless be taken as preliminary evidence that representations of symmetries

174 in wallpaper groups may be compositional.

175 Finally, we conducted a correlation analysis comparing SSVEP and psychophysical data and
176 found a reliable correlation ($R^2 = 0.44$, Bayesian confidence interval [0.28, 0.55]). The correlation
177 reflects an inverse relationship: For subgroup relationships where the supergroup produces a
178 much *larger* SSVEP amplitude than the subgroup, the supergroup also tends to produce a much
179 *smaller* symmetry detection threshold. This is consistent with our hypotheses about how the
180 two measurements relate to symmetry representations in the brain, and suggests that our brain
181 imaging and psychophysical measurements are at least to some extent tapping into the same
182 underlying mechanisms.

183 Discussion

184 Here we show that beyond merely responding to the elementary symmetry operations of reflec-
185 tion (Sasaki et al., 2005; Tyler et al., 2005) and rotation (Kohler et al., 2016), the visual system
186 represents the hierarchical structure of the 17 wallpaper groups, and thus every combination of
187 the four fundamental symmetries (rotation, reflection, translation, glide reflection) which com-
188 prise the set of regular textures. Both SSVEP amplitudes and symmetry detection thresholds
189 preserve the hierarchy of complexity among the wallpaper groups that is captured by the sub-
190 group relationships (Coxeter and Moser, 1972). For the SSVEP, this remarkable consistency was
191 specific to the odd harmonics of the stimulus frequency that are known to capture the symmetry-
192 specific response (Kohler et al., 2016) and to electrodes in a region-of-interest (ROI) over occipital
193 cortex. When the same analysis was done using the odd harmonics from electrodes over parietal
194 cortex (Supplementary Figure 3.3) or even harmonics from electrodes over occipital cortex (Sup-
195 plementary Figure 3.4), the data was substantially less consistent with the subgroup relationships
196 (yellow and green lines, Figure 5).

197 The current study uses 16 distinct wallpaper groups, while previous neuroimaging studies
198 focused on a subset of 4 (Kohler et al., 2016, 2018). This represents a significant conceptual advance,
199 because it makes it possible to investigate the complete subgroup hierarchy among the 17 groups
200 and ask to what extent the hierarchy is reflected in brain activity. Our data provide a description
201 of the visual system's response to the complete set of symmetries in the two-dimensional plane.
202 We do not independently measure the response to P_1 , but because each of the 16 other groups
203 produce non-zero odd harmonic amplitudes (see Figure 2), we can conclude that the relationships
204 between P_1 and all other groups, where P_1 is the subgroup, are also preserved by the visual system.
205 The subgroup relationships are in many cases not obvious perceptually, and most participants
206 had no knowledge of group theory. Thus, the visual system's ability to preserve the subgroup
207 hierarchy does not depend on explicit knowledge of the relationships. Previous brain-imaging
208 studies have found evidence of parametric responses with the number of reflection symmetry folds
209 (Keefe et al. (2018); Sasaki et al. (2005); Makin et al. (2016)) and with the order of rotation symmetry
210 (Kohler et al. (2016)). Our study is the first demonstration that the brain encodes symmetry in
211 this parametric fashion across every possible combination of different symmetry types, and that this
212 parametric encoding is also reflected in behavior. Previous behavioral experiments have shown

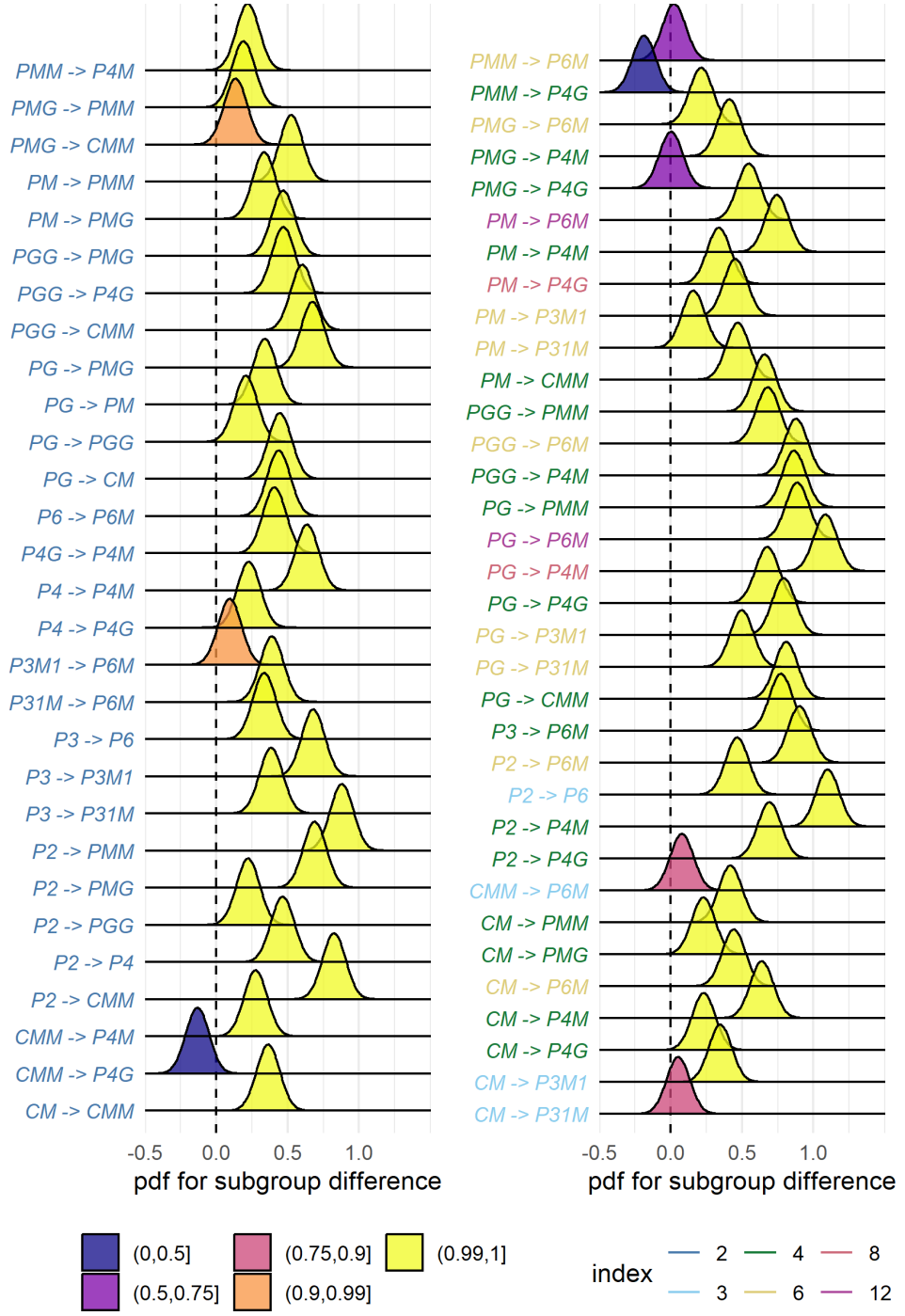


Figure 3: Posterior distributions for the difference in mean SSVEP RMS amplitude. Colour coding of the text indicates the index of the subgroup, while the colour of the filled distribution relates to the conditional probability that the difference in means is greater than zero. We can see that 55/63 subgroup relationships have $p(\Delta < 0 | \text{data}) > 0.99$.

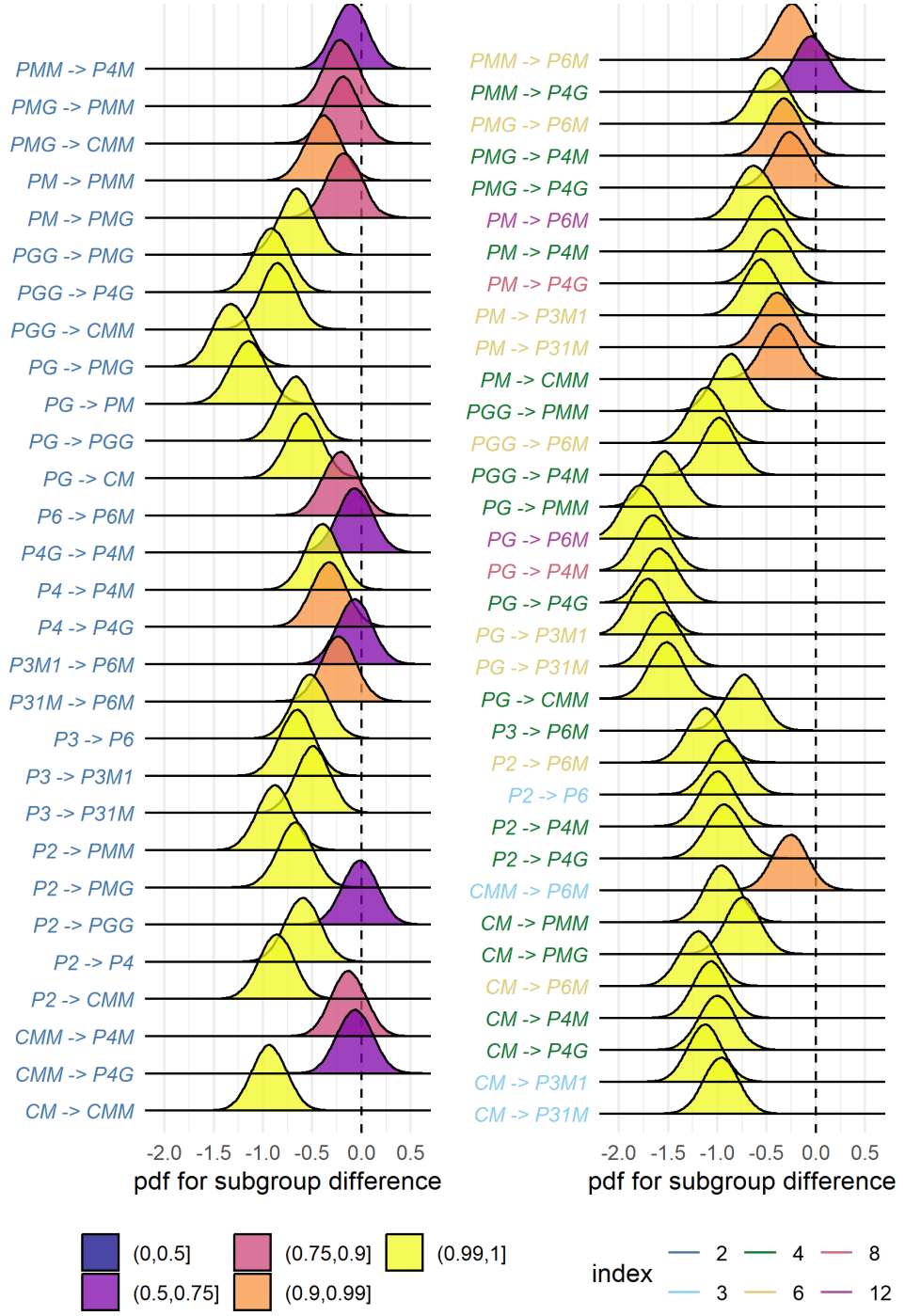


Figure 4: Posterior distributions for the difference in mean symmetry detection threshold durations. Colour coding of the text indicates the index of the subgroup, while the colour of the filled distribution relates to the conditional probability that the difference in means is smaller than zero. We can see that 43/63 subgroup relationships have $p(\Delta > 0 | \text{data}) > 0.99$.

that although naïve observers can distinguish many of the wallpaper groups (Landwehr, 2009), they tend to sort exemplars into fewer (4–12) sets than the number of wallpaper groups, often placing exemplars from different wallpaper groups in the same set (Clarke et al., 2011). The two-interval forced choice approach we use in the current psychophysical experiment makes it possible to directly compare symmetry detection thresholds to the subgroup hierarchy, and reveals that not only can the 17 wallpaper groups be distinguished based on behavioral data, behavior largely follows the subgroup hierarchy.

A large literature exists on the *Sustained Posterior Negativity* (SPN), a characteristic negative-going waveform that is known to reflect responses to symmetry and other forms of regularity and structure (Makin et al., 2016). The SPN scales with the proportion of reflection symmetry in displays that contain a mixture of symmetry and noise Makin et al. (2020); Palumbo et al. (2015), and both reflection, rotation and translation can produce a measurable SPN Makin et al. (2013). It has recently been demonstrated that a holographic model of regularity (van der Helm and Leeuwenberg, 1996), can predict both SPN amplitude (Makin et al., 2016) and perceptual discrimination performance (Nucci and Wagemans, 2007) for dot patterns that contain symmetry and other types of regularity. The available evidence suggests that the SPN and our SSVEP measurements are two distinct methods for isolating the same symmetry-related brain response: When observed in the time-domain, the symmetry-selective odd-harmonic responses produce similarly sustained waveforms (see Figure 2), odd-harmonic SSVEP responses can be measured for dot patterns similar to those used to measure the SPN (Norcia et al., 2002), and the one event-related study on the wallpaper groups also found SPN-like waveforms (Kohler et al., 2018). Future work should more firmly establish the connection and determine if the SPN can capture similarly precise symmetry responses as the SSVEPs presented here. It would also be worthwhile to ask if and how W can be computed for our random-noise based wallpaper textures where combinations of symmetries tile the plane.

We observe a reliable correlation between our brain imaging and psychophysical data. This suggests that the two measurements reflect the same underlying symmetry representations in visual cortex. It should be noted that the correlation is relatively modest ($R^2 = 0.44$). This may be partly due to the fact that different individuals participated in the two experiments. It may also be related to the fact that participants were not doing a symmetry-related task during the SSVEP experiment, but instead monitored the stimuli for brief changes in contrast that occurred twice per trial (see Methods). Previous brain imaging studies have found enhanced reflection symmetry responses when participants performed a symmetry-related task (Makin et al., 2020; Sasaki et al., 2005; Keefe et al., 2018). It is possible that adding a symmetry-related task to our SSVEP experiment would have produced measurements that reflected subgroup relationships to an even higher extent than what we observed. On the other hand, our results are already close to ceiling (see Figure 5) and adding a symmetry-related task may simply enhance SSVEP amplitudes overall without improving the discriminability of individual groups, as has been observed for reflection by Keefe et al. (2018). Task-driven processing may be important for detecting symmetries that have been subject to perspective distortion, as suggested by SPN measurements (Makin et al., 2015) and somewhat less clearly in a subsequent functional MRI study (Keefe et al., 2018).

254 Future work in which behavioral and brain imaging data are collected from the same participants,
255 and task is manipulated in the SSVEP experiment, will help further establish the connection be-
256 tween the two measurements, and elucidate the potential contribution of task-related top-down
257 processing to the current results.

258 We also find an effect of index for both our brain imaging measurements and our symmetry
259 detection thresholds. This means that the visual system not only represents the hierarchical rela-
260 tionship captured by individual subgroups, but also distinguishes between subgroups depending
261 on how many times the subgroup is repeated in the supergroup, with more repetitions leading
262 to larger pairwise differences. Our measured effect of index is relatively weak. This is perhaps
263 because the index analysis does not take into account the *type* of isometries that differentiate the
264 subgroup and supergroup. The effect of symmetry type can be observed by contrasting the mea-
265 sured SSVEP amplitudes and detection thresholds for groups *PM* and *PG* in Figure 2. The two
266 groups are comparable except *PM* contains reflection and *PG* contains glide reflection, and the
267 former clearly elicits higher amplitudes and lower thresholds. An important goal for future work
268 will be to map out how different symmetry types contribute to the representational hierarchy.

269 The correspondence between responses in the visual system and group theory that we demon-
270 strate here, may reflect a form of implicit learning that depends on the structure of the natural
271 world. The environment is itself constrained by physical forces underlying pattern formation
272 and these forces are subject to multiple symmetry constraints (Hoyle, 2006). The ordered struc-
273 ture of responses to wallpaper groups could be driven by a central tenet of neural coding, that of
274 efficiency. If coding is to be efficient, neural resources should be distributed to capture the struc-
275 ture of the environment with minimum redundancy considering the visual geometric optics, the
276 capabilities of the subsequent neural coding stages and the behavioral goals of the organism (At-
277 tneave, 1954; Barlow, 1961; Laughlin, 1981; Geisler et al., 2009). Early work within the efficient
278 coding framework suggested that natural images had a $1/f$ spectrum and that the corresponding
279 redundancy between pixels in natural images could be coded efficiently with a sparse set of ori-
280 ented filter responses, such as those present in the early visual pathway (Field, 1987; Olshausen
281 and Field, 1997). Our results suggest that the principle of efficient coding extends to a much
282 higher level of structural redundancy – that of symmetries in visual images.

283 The 17 wallpaper groups are completely regular, and relatively rare in the visual environment,
284 especially when considering distortions due to perspective (see above) and occlusion. Near-regular
285 textures, however, abound in the visual world, and can be modeled as deformed versions of the
286 wallpaper groups (Liu et al., 2004). The correspondence between visual cortex responses and
287 group theory demonstrated here may indicate that the visual system represents visual textures
288 using a similar scheme, with the wallpaper groups serving as anchor points in representational
289 space. This framework resembles norm-based encoding strategies that have been proposed for
290 other stimulus classes, most notably faces (Leopold et al., 2006), and leads to the prediction that
291 adaptation to wallpaper patterns should distort perception of near-regular textures, similar to
292 the aftereffects found for faces (Webster and MacLin, 1999). Field biologists have demonstrated
293 that animals respond more strongly to exaggerated versions of a learned stimulus, referred to
294 as “supernormal” stimuli (Tinbergen, 1953). In the norm-based encoding framework, wallpaper

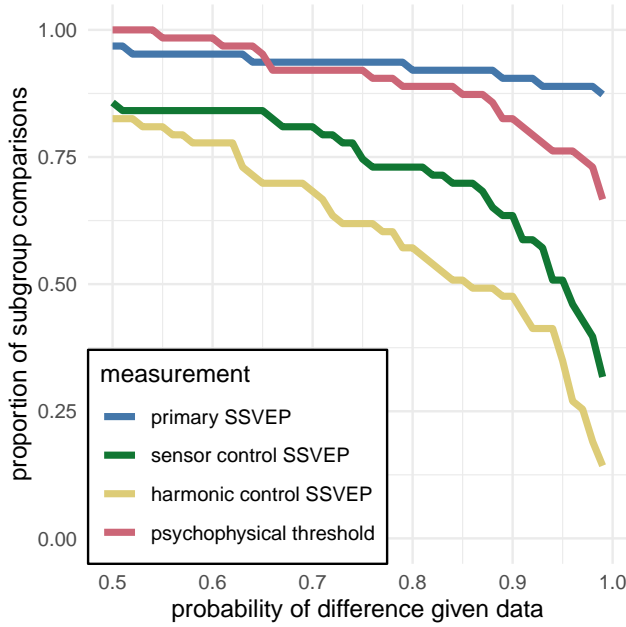


Figure 5: This plot shows the proportion of subgroup relationships that satisfy $p(\Delta > 0 | \text{data}) > x$ for the SSVEP data and $p(\Delta < 0 | \text{data}) > x$ for the psychophysical data. We can see that if we take $x = 0.95$ as our threshold, the subgroup relationships are preserved in $56/63 = 89\%$ and $48/63 = 76\%$ of the comparisons for the primary SSVEP and threshold duration datasets, respectively. This compares to the $32/63 = 51\%$ and $22/63 = 35\%$ for the SSVEP control datasets.

groups can be considered *supertextures*, exaggerated examples of the near-regular textures common in the natural world. If non-human animals employ a similar encoding strategy, they would be expected to be sensitive to symmetries in wallpaper groups. Recent functional MRI work in macaque monkeys offer some support for that: Macaque visual cortex responds parametrically to reflection and rotation symmetries in wallpaper groups, and the set of brain areas involved largely overlap those observed to be sensitive to symmetry in humans (Audurier et al., 2021). In human societies, visual artists may consciously or unconsciously create supernormal stimuli, to capture the essence of the subject and evoke strong responses in the audience (Ramachandran and Hirstein, 1999). Wallpaper groups are visually compelling, and symmetries have been widely used in human artistic expression going back to the Neolithic age (Jablan, 2014). If wallpapers are in fact supertextures, this prevalence may be a direct result of the strategy the human visual system has adopted for texture encoding.

Participants

Twenty-five participants (11 females, mean age 28.7 ± 3.3) took part in the EEG experiment. Their informed consent was obtained before the experiment under a protocol that was approved by the Institutional Review Board of Stanford University. 11 participants (8 females, mean age 20.73 ± 1.21) took part in the psychophysics experiment. All participants had normal or corrected-to-normal vision. Their informed consent was obtained before the experiment under a protocol that was approved by the University of Essex's Ethics Committee. There was no overlap in

314 participants between the EEG and psychophysics experiments.

315 Stimulus Generation

316 Exemplars from the different wallpaper groups were generated using a modified version of the
317 methodology developed by Clarke and colleagues(Clarke et al., 2011) that we have described in de-
318 tail elsewhere(Kohler et al., 2016). Briefly, exemplar patterns for each group were generated from
319 random-noise textures, which were then repeated and transformed to cover the plane, according
320 to the symmetry axes and geometric lattice specific to each group. The use of noise textures as
321 the starting point for stimulus generation allowed the creation of an almost infinite number of
322 distinct exemplars of each wallpaper group. To make individual exemplars as similar as possible
323 we replaced the power spectrum of each exemplar with the median across exemplars within a
324 group. We then generated control exemplars that had the same power spectrum as the exemplar
325 images by randomizing the phase of each exemplar image. The phase scrambling eliminates ro-
326 tation, reflection and glide-reflection symmetries within each exemplar, but the phase-scrambled
327 images inherit the spectral periodicity arising from the periodic tiling. This means that all
328 control exemplars, regardless of which wallpaper group they are derived from, are transformed
329 into another symmetry group, namely P_1 . P_1 is the simplest of the wallpaper groups and contains
330 only translations of a region whose shape derives from the lattice. Because the different wallpaper
331 groups have different lattices, P_1 controls matched to different groups have different power spectra.
332 Our experimental design takes these differences into account by comparing the neural responses
333 evoked by each wallpaper group to responses evoked by the matched control exemplars.

334 Stimulus Presentation

335 Stimulus Presentation. For the EEG experiment, the stimuli were shown on a 24.5" Sony Trima-
336 ster EL PVM-2541 organic light emitting diode (OLED) display at a screen resolution of 1920×1080
337 pixels, 8-bit color depth and a refresh rate of 60 Hz, viewed at a distance of 70 cm. The mean
338 luminance was 69.93 cd/m^2 and contrast was 95%. The diameter of the circular aperture in
339 which the wallpaper pattern appeared was 13.8° of visual angle presented against a mean lumi-
340 nance gray background. Stimulus presentation was controlled using in-house software. For the
341 psychophysics experiment, the stimuli were shown on a $48 \times 27\text{cm}$ VIEWPiXX/3D LCD Display
342 monitor, model VPX-VPX-2005C, resolution 1920×1080 pixels, with a viewing distance of ap-
343 proximately 40cm and linear gamma. Stimulus presentation was controlled using MatLab and
344 Psychtoolbox-3 (Kleiner et al., 2007; Brainard, 1997). The diameter of the circular aperture for
345 the stimuli was 21.5° .

346 EEG Procedure

347 Visual Evoked Potentials were measured using a steady-state design, in which P_1 control images
348 alternated with exemplar images from each of the 16 other wallpaper groups. Exemplar images
349 were always preceded by their matched P_1 control image. A single 0.83 Hz stimulus cycle consisted
350 of a control P_1 image followed by an exemplar image, each shown for 600 ms. A trial consisted of 10

such cycles (12 sec) over which 10 different exemplar images and matched controls from the same rotation group were presented. For each group type, the individual exemplar images were always shown in the same order within the trials. Participants initiated each trial with a button-press, which allowed them to take breaks between trials. Trials from a single wallpaper group were presented in blocks of four repetitions, which were themselves repeated twice per session, and shown in random order within each session. To control fixation, the participants were instructed to fixate a small white cross in the center of display. To control vigilance, a contrast dimming task was employed. Two times per trial, an image pair (*control P₁ plus exemplar*) was shown at reduced contrast. Participants were instructed to press a button on a response pad whenever they noticed a contrast change. Reaction times were not taken into account and participants were told to respond at their own pace while being as accurate as possible. We adjusted the reduction in contrast such that average accuracy for each participant was kept at 85% correct, in order to keep the difficulty of the vigilance task at a constant level.

Psychophysics Procedure

The experiment consisted of 16 blocks, one for each of the wallpaper groups (excluding *P₁*). We used a two-interval forced choice approach. In each trial, participants were presented with two stimuli (one of which was the wallpaper group for the current block of trials, the other being *P₁*), one after the other (inter-stimulus interval of 700ms). After each stimulus had been presented, it was masked with white noise for 300ms. After both stimuli had been presented, participants made a response on the keyboard to indicate whether they thought the first or second image contained more symmetry. Each block started with 10 practice trials, (stimulus display duration of 500ms) to allow participants to familiarise themselves with the current block's wallpaper pattern. If they achieved an accuracy of 9/10 in these trials they progressed to the rest of the block, otherwise they carried out another set of 10 practise trials. This process was repeated until the required accuracy of 9/10 was obtained. The rest of the block consisted of four interleaved staircases (using the QUEST algorithm (Watson and Pelli, 1983), full details given in the SI) of 30 trials each. On average, a block of trials took around 10 minutes to complete.

EEG Acquisition and Preprocessing

Steady-State Visual Evoked Potentials (SSVEPs) were collected with 128-sensor HydroCell Sensor Nets (Electrical Geodesics, Eugene, OR) and were band-pass filtered from 0.3 to 50 Hz. Raw data were evaluated off line according to a sample-by-sample thresholding procedure to remove noisy sensors that were replaced by the average of the six nearest spatial neighbors. On average, less than 5% of the electrodes were substituted; these electrodes were mainly located near the forehead or the ears. The substitutions can be expected to have a negligible impact on our results, as the majority of our signal can be expected to come from electrodes over occipital, temporal and parietal cortices. After this operation, the waveforms were re-referenced to the common average of all the sensors. The data from each 12s trial were segmented into five 2.4 s long epochs (i.e., each of these epochs was exactly 2 cycles of image modulation). Epochs for which a large percentage of data samples exceeding a noise threshold (depending on the participant and ranging between 25

and $50 \mu\text{V}$) were excluded from the analysis on a sensor-by-sensor basis. This was typically the case for epochs containing artifacts, such as blinks or eye movements. Steady-state stimulation will drive cortical responses at specific frequencies directly tied to the stimulus frequency. It is thus appropriate to quantify these responses in terms of both phase and amplitude. Therefore, a Fourier analysis was applied on every remaining epoch using a discrete Fourier transform with a rectangular window. The use of two-cycle long epochs (i.e., 2.4 s) was motivated by the need to have a relatively high resolution in the frequency domain, $\delta f = 0.42 \text{ Hz}$. For each frequency bin, the complex-valued Fourier coefficients were then averaged across all epochs within each trial. Each participant did two sessions of 8 trials per condition, which resulted in a total of 16 trials per condition.

SSVEP Analysis

Response waveforms were generated for each group by selective filtering in the frequency domain. For each participant, the average Fourier coefficients from the two sessions were averaged over trials and sessions. The SSVEP paradigm we used allowed us to separate symmetry-related responses from non-specific contrast transient responses. Previous work has demonstrated that symmetry-related responses are predominantly found in the odd harmonics of the stimulus frequency, whereas the even harmonics consist mainly of responses unrelated to symmetry, that arise from the contrast change associated with the appearance of the second image (Norcia et al., 2002; Kohler et al., 2016). This functional distinction of the harmonics allowed us to generate a single-cycle waveform containing the response specific to symmetry, by filtering out the even harmonics in the spectral domain, and then back-transforming the remaining signal, consisting only of odd harmonics, into the time-domain. For our main analysis, we averaged the odd harmonic single-cycle waveforms within a six-electrode region of interest (ROI) over occipital cortex (electrodes 70, 74, 75, 81, 82, 83). These waveforms, averaged over participants, are shown in Figure 2. The same analysis was done for the even harmonics and for the odd harmonics within a six electrode ROI over parietal cortex (electrodes 53, 54, 61, 78, 79, 86; see Supplementary Figure 1.1). The root-mean square values of these waveforms, for each individual participant, were used to determine whether each of the wallpaper subgroup relationships were preserved in the brain data.

Defining the list of subgroup relationships

In order to get the complete list of subgroup relationships, we digitized Table 4 from Coxeter (Coxeter and Moser, 1972) (shown in Supplementary Table 1.2). After removing identity relationships (i.e. each group is a subgroup of itself) and the three pairs of wallpaper groups that are subgroups of each other (e.g. *PM* is a subgroup of *CM*, and *CM* is a subgroup of *PM*) we were left with a total of 63 unambiguous subgroups that were included in our analysis.

425 Bayesian Analysis of SSVEP and Psychophysical data

426 Bayesian analysis was carried out using R (v3.6.1) (R Core Team, 2019) with the `brms` package
427 (v2.9.0) (Bürkner, 2017) and rStan (v2.19.2 (Stan Development Team, 2019)). The data from each
428 experiment were modelled using a Bayesian generalised mixed effect model with wallpaper group
429 being treated as a 16-level factor, and random effects for participant. The SSVEP data and sym-
430 metry detection threshold durations were modelled using log-normal distributions with weakly
431 informative, $\mathcal{N}(0, 2)$, priors. After fitting the model to the data, samples were drawn from the
432 posterior distribution of the two datasets, for each wallpaper group. These samples were then
433 recombined to calculate the distribution of differences for each of the 63 pairs of subgroup and
434 supergroup. These distributions were then summarised by computing the conditional probabil-
435 ity of obtaining a positive (negative) difference, $p(\Delta|\text{data})$. For further technical details, please
436 see the [Supplementary Materials](#) where the full R code, model specification, prior and posterior
437 predictive checks, and model diagnostics, can be found.

438 References

- 439 Apthorp, D. and Bell, J. (2015). Symmetry is less than $\frac{466}{466}$ meets the eye. *Current Biology*, 25(7):R267–R268.
440
- 441 Attneave, F. (1954). Some informational aspects of $\frac{468}{468}$ visual perception. *Psychol Rev*, 61(3):183–93.
442
- 443 Audurier, P., Héjja-Brichard, Y., Castro, V. $\frac{470}{470}$, Kohler, P. J., Norcia, A. M., Durand, J.-B., and
444 Cottreau, B. R. (2021). Symmetry processing $\frac{472}{472}$ in the macaque visual cortex. *bioRxiv*, page
446 $\frac{473}{473}$ 2021.03.13.435181. Publisher: Cold Spring Harbor
447 Laboratory Section: New Results.
448
- 449 Barlow, H. B. (1961). *Possible principles underlying the $\frac{475}{475}$ transformations of sensory messages*, pages $\frac{217}{217}$ – $\frac{234}{234}$.
450 MIT Press.
451
- 452 Brainard, D. H. (1997). Spatial vision. *The $\frac{478}{478}$ psychophysics toolbox*, 10:433–436.
453
- 454 Bürkner, P.-C. (2017). Advanced bayesian multilevel
455 modeling with the r package brms. *arXiv preprint*
456 *arXiv:1705.11123*.
457 Clarke, A. D. F., Green, P. R., Halley, F., and
458 Chantler, M. J. (2011). Similar symmetries: The
459 role of wallpaper groups in perceptual texture sim-
460 ilarity. *Symmetry*, 3(4):246–264.
461 Cohen, E. H. and Zaidi, Q. (2013). Symmetry in con-
462 text: Salience of mirror symmetry in natural pat-
463 terns. *Journal of vision*, 13(6).
464 Coxeter, H. S. M. and Moser, W. O. J. (1972). *Gen-
465 erators and relations for discrete groups*. Ergebnisse
466 der Mathematik und ihrer Grenzgebiete ; Bd. 14.
467 Springer-Verlag, Berlin, New York.
468 Fedorov, E. (1891). Symmetry in the plane. In *Za-
469 piski Imperatorskogo S. Peterburgskogo Mineralogichesko-
470 g Obshchestva [Proc. S. Peterb. Mineral. Soc.]*, volume 2,
471 pages 345–390.
472 Field, D. J. (1987). Relations between the statistics
473 of natural images and the response properties of
474 cortical cells. *J Opt Soc Am A*, 4(12):2379–94.
475 Geisler, W. S., Najemnik, J., and Ing, A. D. (2009). Opt-
476 imal stimulus encoders for natural tasks. *Journal
477 of Vision*, 9(13):17–17.
478 Giurfa, M., Eichmann, B., and Menzel, R. (1996).
479 Symmetry perception in an insect. *Nature*,
480 382(6590):458–461. Number: 6590 Publisher: Na-
481 ture Publishing Group.
482 Hamada, J. and Ishihara, T. (1988). Complexity and
483 goodness of dot patterns varying in symmetry. *Psy-
484 chological Research*, 50(3):155–161.
485 Hoyle, R. B. (2006). *Pattern formation: an introduction
486 to methods*. Cambridge University Press.
487 Jablan, S. V. (2014). *Symmetry, Ornament and Modular-
488 ity*. World Scientific Publishing Co Pte Ltd, Singa-
489 pore, SINGAPORE.

- Keefe, B. D., Gouws, A. D., Sheldon, A. A., Vernon, R. J. W., Lawrence, S. J. D., McKeefry, D. J., Wade, A. R., and Morland, A. B. (2018). Emergence of symmetry selectivity in the visual areas of the human brain: fMRI responses to symmetry presented in both frontoparallel and slanted planes. *Human Brain Mapping*, 39(10):3813–3826.
- Kleiner, M., Brainard, D., Pelli, D., Ingling, A., Murray, R., and Broussard, C. (2007). What's new in psychtoolbox-3. *Perception*, 36:1–16.
- Kohler, P. J., Clarke, A., Yakovleva, A., Liu, Y., and Norcia, A. M. (2016). Representation of maximally regular textures in human visual cortex. *The Journal of Neuroscience*, 36(3):714–729.
- Kohler, P. J., Cottreau, B. R., and Norcia, A. M. (2018). Dynamics of perceptual decisions about symmetry in visual cortex. *NeuroImage*, 167(Supplement C):316–330.
- Landwehr, K. (2009). Camouflaged symmetry. *Perception*, 38:1712–1720.
- Laughlin, S. (1981). A simple coding procedure enhances a neuron's information capacity. *Z Naturforsch C*, 36(9-10):910–2.
- Leopold, D. A., Bondar, I. V., and Giese, M. A. (2006). Norm-based face encoding by single neurons in the monkey inferotemporal cortex. *Nature*, 442(7102):572–5.
- Li, Y., Sawada, T., Shi, Y., Steinman, R., and Pizlo, Z. (2013). *Symmetry Is the sine qua non of Shape*, book section 2, pages 21–40. Advances in Computer Vision and Pattern Recognition. Springer London.
- Liu, Y., Hel-Or, H., Kaplan, C. S., and Van Gool, L. (2010). Computational symmetry in computer vision and computer graphics. *Foundations and Trends® in Computer Graphics and Vision*, 5(1–2):1–195.
- Liu, Y., Lin, W.-C., and Hays, J. (2004). Near-regular texture analysis and manipulation. In *ACM Transactions on Graphics (TOG)*, volume 23, pages 368–376. ACM.
- Mach, E. (1959). *The Analysis of Sensations* (1897; English transl., Dover, New York).
- Makin, A. D. J., Rampone, G., and Bertamini, M. (2015). Conditions for view invariance in the neural response to visual symmetry. *Psychophysiology*, 52(4):532–543. eprint: <https://onlinelibrary.wiley.com/doi/pdf/10.1111/psyp.12365>.
- Makin, A. D. J., Rampone, G., Morris, A., and Bertamini, M. (2020). The Formation of Symmetrical Gestalts Is Task-Independent, but Can Be Enhanced by Active Regularity Discrimination. *Journal of Cognitive Neuroscience*, 32(2):353–366.
- Makin, A. D. J., Rampone, G., Pecchinenda, A., and Bertamini, M. (2013). Electrophysiological responses to visuospatial regularity. *Psychophysiology*, 50(10):1045–1055. eprint: <https://onlinelibrary.wiley.com/doi/pdf/10.1111/psyp.12082>.
- Makin, A. D. J., Rampone, G., Wright, A., Martinovic, J., and Bertamini, M. (2014). Visual symmetry in objects and gaps. *Journal of Vision*, 14(3):12–12. Publisher: The Association for Research in Vision and Ophthalmology.
- Makin, A. D. J., Wilton, M. M., Pecchinenda, A., and Bertamini, M. (2012). Symmetry perception and affective responses: A combined EEG/EMG study. *Neuropsychologia*, 50(14):3250–3261.
- Makin, A. D. J., Wright, D., Rampone, G., Palumbo, L., Guest, M., Sheehan, R., Cleaver, H., and Bertamini, M. (2016). An Electrophysiological Index of Perceptual Goodness. *Cerebral Cortex*, 26(12):4416–4434.
- Morris, M. R. and Casey, K. (1998). Female swordtail fish prefer symmetrical sexual signal. *Animal Behaviour*, 55(1):33–39.
- Møller, A. P. (1992). Female swallow preference for symmetrical male sexual ornaments. *Nature*, 357(6375):238–240.
- Norcia, A. M., Appelbaum, L. G., Ales, J. M., Cottreau, B. R., and Rossion, B. (2015). The steady-state visual evoked potential in vision research: A review. *Journal of Vision*, 15(6):4–4.
- Norcia, A. M., Candy, T. R., Pettet, M. W., Vildavski, V. Y., and Tyler, C. W. (2002). Temporal dynamics of the human response to symmetry. *Journal of Vision*, 2(2):132–139.

- 575 Nucci, M. and Wagemans, J. (2007). Goodness of
 576 Regularity in Dot Patterns: Global Symmetry, Local
 577 Symmetry, and Their Interactions. *Perception*,
 578 36(9):1305–1319. Publisher: SAGE Publications
 579 Ltd STM. 620
- 580 Ogden, R., Makin, A. D. J., Palumbo, L., and
 581 Bertamini, M. (2016). Symmetry Lasts Longer
 582 Than Random, but Only for Brief Presentations.
 583 *i-Perception*, 7(6):2041669516676824. Publisher:
 584 SAGE Publications. 624
- 585 Olshausen, B. A. and Field, D. J. (1997). Sparse coding
 586 with an overcomplete basis set: a strategy em-
 587 ployed by v1? *Vision Res*, 37(23):3311–25. 627
- 588 Palmer, S. E. (1985). The role of symmetry in shape
 589 perception. *Acta Psychologica*, 59(1):67–90. 630
- 590 Palmer, S. E. (1991). Goodness, Gestalt, groups, and
 591 Garner: Local symmetry subgroups as a theory
 592 of figural goodness. In *The perception of structure*:
 593 *Essays in honor of Wendell R. Garner*, pages 23–30.
 594 American Psychological Association, Washington,
 595 DC, US. 635
- 596 Palumbo, L., Bertamini, M., and Makin, A. (2015).
 597 Scaling of the extrastriate neural response to sym-
 598 metry. *Vision Research*, 117:1–8. 638
- 599 Polya, G. (1924). Xii. Über die analogie der
 600 kristallsymmetrie in der ebene. *Zeitschrift für*
 601 *Kristallographie-Crystalline Materials*, 60(1):278–282. 639
- 602 R Core Team (2019). *R: A Language and Environment
 603 for Statistical Computing*. R Foundation for Statisti-
 604 cal Computing, Vienna, Austria. 645
- 605 Ramachandran, V. S. and Hirstein, W. (1999). The
 606 science of art: A neurological theory of aesthetic
 607 experience. *Journal of Consciousness Studies*, 6(6–
 608 7):15–41. 648
- 609 Rhodes, G., Proffitt, F., Grady, J. M., and Sumich-
 610 A. (1998). Facial symmetry and the perception of
 611 beauty. *Psychonomic Bulletin & Review*, 5(4):650–
 612 669. 653
- 613 Royer, F. L. (1981). Detection of symmetry. *Journal
 614 of Experimental Psychology: Human Perception and
 615 Performance*, 7(6):1186–1210. 654
- Sasaki, Y., Vanduffel, W., Knutson, T., Tyler, C., and
 Tootell, R. (2005). Symmetry activates extrastriate
 visual cortex in human and nonhuman primates.
*Proceedings of the National Academy of Sciences of the
 United States of America*, 102(8):3159–3163.
- Schlüter, A., Parzefall, J., and Schlupp, I. (1998). Fe-
 male preference for symmetrical vertical bars in
 male sailfin mollies. *Animal Behaviour*, 56(1):147–
 153.
- Stan Development Team (2019). RStan: the R inter-
 face to Stan. R package version 2.19.2.
- Swaddle, J. P. (1999). Visual signalling by asymme-
 try: a review of perceptual processes. *Philosophical
 Transactions of the Royal Society of London. Series B:
 Biological Sciences*. Publisher: The Royal Society.
- Swaddle, J. P. and Cuthill, I. C. (1994). Preference for
 symmetric males by female zebra finches. *Nature*,
 367(6459):165–166. Number: 6459 Publisher: Na-
 ture Publishing Group.
- Tinbergen, N. (1953). *The herring gull's world: a study
 of the social behaviour of birds*. Frederick A. Praeger,
 Inc., Oxford, England.
- Tyler, C. W., Baseler, H. A., Kontsevich, L. L.,
 Likova, L. T., Wade, A. R., and Wandell, B. A.
 (2005). Predominantly extra-retinotopic corti-
 cal response to pattern symmetry. *Neuroimage*,
 24(2):306–314.
- van der Helm, P. A. and Leeuwenberg, E. L. J. (1996).
 Goodness of visual regularities: A nontransfor-
 mational approach. *Psychological Review*, 103(3):429–
 456. Publisher: American Psychological Associa-
 tion.
- von Fersen, L., Manos, C. S., Goldowsky, B., and Roit-
 blat, H. (1992). Dolphin Detection and Conceptu-
 alization of Symmetry. In Thomas, J. A., Kastelein,
 R. A., and Supin, A. Y., editors, *Marine Mammal Sen-
 sory Systems*, pages 753–762. Springer US, Boston,
 MA.
- Wagemans, J. (1998). Parallel visual processes in sym-
 metry perception: Normality and pathology. *Doc-
 umenta Ophthalmologica*, 95(3):359.

- 657 Wagemans, J., Van Gool, L., and d'Ydewalle, G.⁶⁵ Webster, M. A. and MacLin, O. H. (1999). Figural
658 (1991). Detection of symmetry in tachistoscopes⁶⁶ aftereffects in the perception of faces. *Psychon Bull*
659 ically presented dot patterns: effects of multi-⁶⁶ Rev, 6(4):647–53.
- 660 ple axes and skewing. *Perception & Psychophysics*,⁶⁶⁸
661 50(5):413–27.
- 662 Wright, D., Makin, A. D. J., and Bertamini, M.⁶⁶⁹
663 Watson, A. B. and Pelli, D. G. (1983). Quest: A⁶⁷⁰ (2015). Right-lateralized alpha desynchronization
664 bayesian adaptive psychometric method. *Percep-⁶⁷¹ during regularity discrimination: Hemispheric
665 tion & Psychophysics*, 33(2):113–120. specialization or directed spatial attention?⁶⁷² *Psychophysiology*, 52(5):638–647. eprint:
666 https://onlinelibrary.wiley.com/doi/pdf/10.1111/psyp.12399.